Journal of Molecular Structure 1106 (2016) 416–423

Contents lists available at ScienceDirect

Journal of Molecular Structure

journal homepage: http://www.elsevier.com/locate/molstruc

Synthesis, spectroscopy and computational studies of some novel π-conjugated vinyl *N*-alkylated quinolinium salts and their precursor's

Jacek E. Nycz [a, *], Karolina Czyż [a], Marcin Szala [a], Jan G. Malecki [a], George Shaw [b], Brendan Gilmore [b], Marek Jon [c]

[a] Institute of Chemistry, University of Silesia, ul. Szkolna 9, PL-40007, Katowice, Poland
[b] School of Pharmacy, The Queens University of Belfast, Medical Biology Centre, 97 Lisburn Road, Belfast, BT9 7BL, UK
[c] Faculty of Chemistry, University of Wrocław, 14 Joliot-Curie Street, 50-383, Wrocław, Poland

ARTICLE INFO

Article history:
Received 30 July 2015
Received in revised form
12 September 2015
Accepted 9 November 2015
Available online 14 November 2015

Keywords:
Quinoline
Vinyl quinolinium salt
Styryl quinolinium salt
Quinolinium salt
Spiro
Perkin condensation
Styryl dye

ABSTRACT

A series of π-conjugated vinyl *N*-methylated quinolinium salts (**3**) and their precursor's *N*-alkylated quinolinium salts (**2**) were prepared and characterized by NMR, IR, UV–Vis and MS spectroscopy. It was confirmed that the hydroxyl and amino derivatives of vinyl *N*-methylated quinolinium salts lead to spiro type compounds (**4**). The syntheses of *N*-alkylated quinolinium salts were successful, and even multigram scale was achievable. The structures of 1,2–dimethylquinolinium iodide (**2a**) and 1-ethyl-2-methylquinolinium iodide (**2b**) were determined by single crystal X-ray diffraction method. NMR spectra showed readily diagnostic H-1 and C-13 signals from methyl and *N*-alkyl groups for both **2** and **3**. The geometries of the studied compounds were optimized in singlet states using the density functional theory (DFT) method with B3LYP functional. In general, the predicted bond lengths and angles are in a good agreement with the values based on the X-ray crystal structure data.

1. Introduction

The quinolinium salts is a class of readily available compounds. Similarly to other heteroarenium salts they possess nitrogen atom with formal positive charge, where lone pair is connected with proton, alkyl, aryl or other functional groups. The compounds have increased water solubility due to their ionic form. Salts of cationic alkaloids possessing pyridinium, quinolinium, and isoquinolinium rings are widespread in nature, such as Berberine, Papaverinium chloride, Thalifedine, Fissisaine or Fenfangjines D [1]. Quinolinium salts and related π-conjugated vinyl *N*-alkylated quinolinium salts were used as DNA fluorescence sensor [2]. *N*-methylquinolinium salts have been used as sensitive fluorescent indicators of many anions, including biologically important intracellular chloride anion [3]. The comparison of different anions suggests that the quenching efficiency is related to the ease of anion oxidation. The quenching mechanism possibly involves charge transfer from the anion to the indicator [3,4]. The quinolinium salts have also been used to stabilize reactive anionic species and used as anion sensors [5,6]. Some of them such as 1,3–dialkylimidazolium or 1–alkylpyridinium compounds exhibited toxicity towards algae, bacteria or fungi [7,8]. It was studied that pyridinium salts underwent a unique cyclization reaction to produce bicyclicaziridines with modest to high efficiency [9], and related isoquinolinium-3-oxides or imines reacted in a similar manner [9]. The same process was found to take place in complex and naturally occurring systems, which was demonstrated by the transformation of berberinephenolbetaines to cycloberberines [10]. This finding suggests that the photoreaction of some heteroarylium salts have high synthetic potential which could lead to interesting structurally and stereochemically complex substances. Formal positive charge on nitrogen atom makes pyridine ring in quinolinium salt constitution more susceptible to nucleophiles attack, especially in 2 and/or 4 positions [11]. This process involved a cation-π interaction, which played a crucial role in the recognition of ligands in biochemical processes and in the formation of the tertiary structure of proteins [12–14]. It also is one of the key forces for the construction of various host–guest complexes and supramolecules [15]. By considering the present knowledge of quinolinium salts, it is

* Corresponding author.
E-mail address: jacek.nycz@us.edu.pl (J.E. Nycz).

http://dx.doi.org/10.1016/j.molstruc.2015.11.011
0022-2860/

conceivable that further explorations on quinolinium salts and the derivatives of vinyl *N*-alkylated quinolinium salts may lead to new applications. Despite the potential value of vinyl *N*-alkylated quinolinium salts, there are only limited examples of vinyl *N*-alkylated quinolinium salts, often without NMR characteristics, to the best of our knowledge according to literature data.

In a series of experiments we obtained five quinolinium salts and eight vinyl *N*-methylated quinolinium salts. Additionally we proved the tendency of the rearrangements of vinyl *N*-methylated quinolinium salts to spiro type compounds, especially the ones with hydroxyl and amino substituents on phenyl ring. This finding could explain the lack of this type of compounds and their poor biological activity. We reported some new approaches for the synthesis of the aforementioned compounds with in-depth spectroscopic characterization. Additionally we carried out computational and X-ray studies to compare the atomic charges of selected quinolinium salts, the energy of the frontier orbitals and the conformation of groups, which have not been determined by crystallographic studies yet.

2. Experimental

2.1. General

Commercially available chemicals and solvents were used without further purification. The ^{1}H and ^{13}C NMR calculations were performed with the ACD Labs NMR Predictor v.12 program considering the influence of different solvents. 2-Methylquinolin-8-ol (**1a**) was purchased from Aldrich, and quinolin-8-ol from Maybridge and were crystallisated before used. The synthesis of 8-methoxyquinoline (**1b**) followed our procedure described in the literature [18] and for *N*-alkylated quinolinium salts **2a**, **2b**, **2c**, **2d** and **2e** [16,17,22,23].

2.2. Synthesis of N-alkylated quinolinium salts

Appropriate RI (R = CH_3, Et, $CH_2CH{=}CH_2$, Bu^i) (1.20 mol) was added to the **1a** or **1b** (0.60 mol) at room temperature. After the completion of addition, the reaction mixture was heated under reflux for 16 h. The excess of RI was slowly evaporated at room temperature. The crude product was purified by crystallization from ethanol (or methanol) and dried over P_4O_{10} to yield precipitates as follows:

1,2–Dimethylquinolinium iodide (**2a**) (yellow) 128.25 g (0.450 mol, 75%); m.p. = 184–185 °C; ^{1}H NMR (DMSO–d_6; 400.2 MHz) δ = 3.11 (s, 3H, CH_3), 4.47 (s, 3H, NCH_3), 7.99 (t, *J* = 7.3 Hz, 1H, aromatic), 8.15 (d, *J* = 8.6 Hz, 1H, aromatic), 8.24 (ddd, *J* = 8.9, 7.0 Hz, J_{HH} = 1.5 Hz 1H, aromatic), 8.42 (dd, *J* = 8.1, 1.2 Hz, 1H, aromatic), 8.61 (d, *J* = 9.0 Hz, 1H, aromatic), 9.13 (d, *J* = 8.6 Hz, 1H, aromatic); $^{13}C\{^{1}H\}$ NMR (DMSO–*d6*; 100.6 MHz) δ = 23.09, 39.73, 118.89, 125.02, 127.65, 128.86, 130.17, 134.92, 139.06, 145.26, 161.02; lit. [22]; UV–Vis (methanol; λ [nm] (logε)): 320 (3.68), 239 (4.23), 220 (4.05), 204 (4.24); IR (KBr): 3045ν_{ArH}; 2986ν_{CH}; 2916ν_{CH}; 1604$\nu_{C=C}$; 1582$\nu_{C=N}$; X-ray CCDC 795822; LCMS-IT-TOF $[M-I]^+$ = 158 (100%), HRMS (IT TOF): m/z Calcd for $C_{11}H_{12}N$-127^+ $[M-I]^+$: 158.09697 Found 158.0964.

1-Ethyl-2–methylquinolinium iodide (**2b**) (yellow) 127.37 g (0.426 mol, 71%); m.p. = 224–225 °C; ^{1}H NMR (DMSO–d_6; 400.2 MHz) δ = 1.56 (t, *J* = 7.3 Hz, 3H, CH_3), 3.14 (s, 3H, CH_3), 5.02 (q, J_{HH} = 7.3 Hz, 2H, NCH_2), 8.01 (t, *J* = 7.5 Hz, 1H, aromatic), 8.15 (d, *J* = 8.6 Hz, 1H, aromatic), 8.25 (ddd, *J* = 8.8, 7.1, 1.5 Hz 1H, aromatic), 8.44 (dd, *J* = 8.1, 1.2 Hz, 1H, aromatic), 8.64 (d, *J* = 9.0 Hz, 1H, aromatic), 9.13 (d, *J* = 8.5 Hz, 1H, aromatic); $^{13}C\{^{1}H\}$ NMR (DMSO–d_6; 100.6 MHz) δ = 13.35, 22.33, 47.12, 118.76, 125.45, 128.13, 128.90, 130.51, 135.16, 137.93, 145.48, 160.40; lit. [23]; UV–Vis (methanol; λ [nm] (logε)): 320 (3.68), 240 (4.25), 220 (4.06), 204 (4.24); IR (KBr): 3059ν_{ArH}; 2924ν_{CH}; 1602$\nu_{C=C}$; 1579$\nu_{C=N}$; X-ray CCDC 873830; LCMS-IT-TOF $[M-I]^+$ = 172 (100%), HRMS (IT TOF): m/z Calcd for $C_{12}H_{14}N$-127^+ $[M-I]^+$: 172.1126, Found 172.1120.

2-Methyl-1-(2-methylpropyl)quinolinium iodide (**2c**) (beige) 27.47 g (0.084 mol, 14%); m.p. = 181.1 °C; ^{1}H NMR (DMSO–d_6; 400.2 MHz) δ = 0.98 (bs, 6H, $CH_2CH(CH_3)_2$), 2.29–2.41 (m, 1H, $CH_2CH(CH_3)_2$), 3.13 (s, 3H, CH_3), 4.88 (bs, 2H, $NCH_2CH(CH_3)_2$), 7.99 (t, *J* = 7.5 Hz, 1H, aromatic), 8.14 (d, *J* = 8.6 Hz, 1H, aromatic), 8.21 (ddd, *J* = 8.9, 7.0, 1.5 Hz 1H, aromatic), 8.42 (dd, *J* = 8.1, 1.4 Hz, 1H, aromatic), 8.64 (d, *J* = 9.1 Hz, 1H, aromatic), 9.13 (d, *J* = 8.5 Hz, 1H, aromatic); $^{13}C\{^{1}H\}$ NMR (DMSO–d_6; 125.78 MHz) δ = 19.26, 23.30, 28.65, 56.91, 119.64, 125.66, 128.34, 129.11, 130.66, 134.98, 138.72, 145.85, 161.22; UV–Vis (methanol; λ [nm] (logε)): 320 (3.54), 241 (4.12), 219 (4.04), 203 (4.22); IR (KBr): 3097ν_{ArH}; 2957ν_{CH}; 1618$\nu_{C=C}$; 1598$\nu_{C=N}$; LCMS-IT-TOF $[M-I]^+$ = 200 (100%), HRMS (IT TOF): m/z Calcd for $C_{14}H_{18}N$-127^+ $[M-I]^+$: 200.1439, Found 200.1433.

8–Methoxy–1–methylquinolinium iodide (**2d**) (greenish) 9.03 g (0.030 mol, 5%); m.p. = 129–130 °C; ^{1}H NMR (DMSO-d_6; 400.2 MHz) δ = 4.08 (s, 3H, OCH_3), 4.79 (s, 3H, NCH_3), 7.74 (dd, *J* = 7.3, 1.6 Hz, 1H, aromatic), 7.92 (m, 2H, aromatic), 8.08 (dd, *J* = 8.3, 5.8 Hz, 1H, aromatic), 9.14 (d, *J* = 8.3 Hz, 1H, aromatic), 9.28 (d, *J* = 5.7 Hz, 1H, aromatic); $^{13}C\{^{1}H\}$ NMR (DMSO-d_6; 100.6 MHz) δ = 52.35, 57.78, 116.73, 122.45, 122.60, 130.79, 130.82, 132.10, 147.48, 151.74, 152.18; UV–Vis (methanol; λ [nm] (logε)): 461 (3.14), 257 (4.41), 222 (3.65), 204 (4.18); IR (KBr): 3097ν_{ArH}; 2955ν_{CH}; 2853ν_{CH}; 1598$\nu_{C=C}$; 1536$\nu_{C=N}$; 1049ν_{O-CH3}; LCMS-IT-TOF $[M-I]^+$ = 174 (100%), HRMS (IT TOF): m/z Calcd for $C_{11}H_{12}NO$-127^+ $[M-I]^+$: 174.0919, Found 174.0913.

2-methyl-1-(prop-2-en-1-yl)quinolinium iodide (**2e**) (greenish) 145.55 g (0.468 mol, 78%); m.p. = 160 °C; ^{1}H NMR (DMSO-d_6; 400.2 MHz) δ = 3.07 (s, 3H, CH_3), 4.98 (d, *J* = 17.4 Hz, 1H, CH), 5.34 (d, *J* = 10.7 Hz, 1H, CH), 5.67 (m, 2H, NCH_2), 6.20 (m, 1H, CH), 7.99 (t, *J* = 7.5 Hz, 1H, aromatic), 8.21 (m, 2H, aromatic), 8.44 (d, *J* = 7.4 Hz, 1H, aromatic), 8.48 (d, *J* = 9.0 Hz, 1H, aromatic), 9.18 (d, *J* = 8.5 Hz, 1H, aromatic); $^{13}C\{^{1}H\}$ NMR (DMSO-d_6; 100.6 MHz) δ = 22.39, 53.58, 118.49, 119.11, 125.49, 128.20, 129.10, 130.05, 130.52, 135.31, 138.60, 146.31, 161.15; UV–Vis (methanol; λ [nm] (logε)): 321 (3.52), 239 (4.08), 219 (3.89), 204 (4.12); IR (KBr): 3035ν_{ArH}; 2925ν_{CH}; 1603$\nu_{C=C}$; 1525$\nu_{C=N}$; LCMS-IT-TOF $[M-I]^+$ = 184 (100%), HRMS (IT TOF): m/z Calcd for $C_{13}H_{14}N$-127^+ $[M-I]^+$: 184.1126, Found 184.1120.

2.3. Synthesis of vinyl N-methylated quinolinium salts. Method A

2a (10.0 g, 35.1 mmol) was partially dissolved in Ac_2O (100 mL, 108 g, 1.06 mol), followed by the addition of appropriate benzaldehyde (50 mmol). The reaction was heated under reflux for 16 h, and was filtered after completion. The solvent was evaporated from the resulting solution. The crude product was purified by crystallization from ethanol (or methanol) and dried over P_4O_{10} to yield precipitates as follows:

2-[(*E*)-2-(2-chlorophenyl)vinyl]-1-methylquinolinium iodide (**3a**) (black) 1.856 g (4.56 mmol, 13%); m.p. = 246 °C; ^{1}H NMR (DMSO-d_6; 400.2 MHz) δ = 4.60 (s, 3H, NCH_3), 7.55 (m, 2H, aromatic), 7.64 (m, 1H, aromatic), 8.01 (t, *J* = 7.5 Hz, 1H, aromatic), 8.02 (d, *J* = 15.5 Hz, 1H, vinyl), 8.16 (d, *J* = 15.9 Hz, 1H, vinyl), 8.25 (m, 2H, aromatic), 8.43 (dd, *J* = 8.1, 1.3 Hz, 1H, aromatic), 8.59 (d, *J* = 8.8 Hz, 1H, aromatic), 8.61 (d, *J* = 9.0 Hz, 1H, aromatic), 9.16 (d, *J* = 8.8 Hz, 1H, aromatic); $^{13}C\{^{1}H\}$ NMR (DMSO-d_6; 125.78 MHz) δ = 40.45, 119.42, 121.88, 123.05, 127.86, 128.24, 129.05, 129.35, 130.15, 130.20, 132.47, 132.56, 134.08, 135.30, 139.21, 140.61, 145.19, 155.64; UV–Vis (methanol; λ [nm] (logε)): 354 (3.92), 292 (3.68), 244 (4.05), 218 (4.24), 204 (4.39); IR (KBr): 3063ν_{ArH}; 2960ν_{CH}; 1608$\nu_{C=C}$; 1585$\nu_{C=N}$; LCMS-IT-TOF $[M-I]^+$ = 280 (100%), HRMS (IT TOF): m/z Calcd for

$C_{18}H_{15}NCl\text{-}127^+$ $[M-I]^+$: 280.0893, Found 280.0887.

2-[(*E*)-2-(4-chlorophenyl)vinyl]-1-methylquinolinium iodide (**3b**) (black) 1.856 g (4.56 mmol, 13%); m.p. = 171 °C; ^1H NMR (DMSO-d_6; 400.2 MHz) δ = 4.59 (s, 3H, NCH_3), 7.64 (d, J = 8.4 Hz, 2H, aromatic), 8.00 (m, 4H aromatic), 8.19 (d, J = 16.2 Hz, 1H, vinyl), 8.22 (m, 1H, vinyl), 8.39 (d, J = 7.9 Hz, 1H, aromatic), 8.57 (d, J = 8.7 Hz, 1H, aromatic), 8.59 (d, J = 8.7 Hz, 1H, aromatic), 9.13 (d, J = 8.9 Hz, 1H, aromatic); $^{13}C\{^1H\}$ NMR (DMSO-d_6; 125.78 MHz) δ = 40.13, 119.39, 120.25, 121.24, 127.98, 129.19, 129.21, 130.12, 130.76, 133.75, 135.07, 135.89, 139.21, 144.48, 145.19, 155.94; UV–Vis (methanol; λ [nm] (logε)): 377 (3.87), 300 (3.63), 247 (3.90), 211 (4.17), 204 (4.19); IR (KBr): 3060ν_{ArH}; 3012ν_{CH}; 1603$\nu_{C=C}$; 1571$\nu_{C=N}$; LCMS-IT-TOF $[M-I]^+$ = 280 (100%); HRMS (IT TOF): m/z Calcd for $C_{18}H_{15}NCl\text{-}35^+$ $[M-I]^+$: 280.0893, Found 280.0891.

2-[(*E*)-2-(4-bromophenyl)vinyl]-1-methylquinolinium iodide (**3c**) (black) 8.865 g (19.66 mmol, 56%); m.p. = 227.6 °C; ^1H NMR (DMSO-d_6; 400.2 MHz) δ = 4.59 (s, 3H, NCH_3), 7.77 (d, J = 8.4 Hz, 2H, aromatic), 7.92–8.01 (m, 3H, aromatic), 8.00 (d, J = 16.0 Hz, 1H, vinyl), 8.18 (d, J = 15.9 Hz, 1H, vinyl), 8.23 (d, J = 7.5 Hz, 1H, aromatic), 8.39 (d, J = 8.0 Hz, 1H, aromatic), 8.58 (d, J = 8.8 Hz, 1H, aromatic), 8.59 (d, J = 8.8 Hz, 1H, aromatic), 9.13 (d, J = 8.9 Hz, 1H, aromatic); $^{13}C\{^1H\}$ NMR (DMSO-d_6; 125.78 MHz) δ = 41.18, 119.43, 120.34, 121.28, 124.89, 128.00, 129.20, 130.12, 131.81, 131.72, 134.11, 135.08, 139.23, 144.48, 145.29, 155.97; UV–Vis (methanol; λ [nm] (logε)): 378 (4.24), 301 (3.88), 247 (4.10), 209 (4.39), 204 (4.40); IR (KBr): 3050ν_{ArH}; 3023ν_{CH}; 1607$\nu_{C=C}$; 1574$\nu_{C=N}$; LCMS-IT-TOF $[M-I]^+$ = 324 (100%), HRMS (IT TOF): m/z Calcd for $C_{18}H_{15}NBr\text{-}127^+$ $[M-I]^+$: 324.0388, Found 324.0382.

2-[(*E*)-2-(4-methoxyphenyl)ethenyl]-1-methylquinolinium iodide (**3d**) (purple) 4.385 g (10.88 mmol, 31%); m.p. = 230.5 °C; ^1H NMR (DMSO-d_6; 400.2 MHz) δ = 3.86 (s, 3H, NCH_3), 4.54 (s, 3H, CH_3), 7.11 (d, J = 8.7 Hz, 2H, aromatic), 7.79 (d, J = 15.8 Hz, 1H, vinyl), 7.90–8.00 (m, 3H, aromatic), 8.17 (dt, J = 7.4, 1.2 Hz, 1H, aromatic), 8.22 (d, J = 15.8 Hz, 1H, vinyl), 8.34 (d, J = 7.3 Hz, 1H, aromatic), 8.55 (t, J = 8.8 Hz, 2H, aromatic), 9.01 (d, J = 9.0 Hz, 1H, aromatic); $^{13}C\{^1H\}$ NMR (DMSO-d_6; 125.78 MHz) δ = 39.78, 55.63, 114.74, 116.58, 119.29, 120.83, 127.57, 127.66, 128.82, 130.04, 131.42, 134.75, 139.20, 143.64, 147.18, 156.38, 162.19; lit. [24]; UV–Vis (methanol; λ [nm] (logε)): 415 (4.10), 288 (3.77), 257 (3.88), 216 (4.20), 203 (4.18); IR (KBr): 3068ν_{ArH}; 2955ν_{CH}; 2832ν_{CH}; 1745$\nu_{C=C}$; 1588$\nu_{C=N}$; 1173ν_{O-CH3}; LCMS-IT-TOF $[M-I]^+$ = 276 (100%), HRMS (IT TOF): m/z Calcd for $C_{19}H_{18}NO\text{-}127^+$ $[M-I]^+$: 276.1388, Found 276.1382.

1-methyl-2-[(*E*)-2-(4-nitrophenyl)ethenyl]quinolinium iodide (**3e**) 11.444 g (27.38 mmol, 78%); m.p. = 243.5 °C; ^1H NMR (DMSO-d_6; 400.2 MHz) δ = 4.64 (s, 3H, NCH_3), 8.02 (t, J = 7.5 Hz, 1H, aromatic), 8.18 (d, J = 16.1 Hz, 1H, vinyl), 8.26 (m, 4H, 3H aromatic and 1H vinyl), 8.38 (d, J = 8.7 Hz, 2H, aromatic), 8.42 (d, J = 8.0 Hz, 1H, aromatic), 8.62 (t, J = 8.6 Hz, 2H, aromatic), 9.20 (d, J = 8.8 Hz, 1H, aromatic); $^{13}C\{^1H\}$ NMR (DMSO-d_6; 125.78 MHz) δ = 40.48, 119.53, 121.62, 123.77, 124.17, 128.33, 129.49, 130.01, 130.19, 135.35, 139.27, 140.98, 143.45, 145.03, 148.33, 155.50; UV–Vis (methanol; λ [nm] (logε)): 368 (4.18), 298 (3.89), 253 (3.70), 217 (4.12), 204 (4.21); IR (KBr): 3065ν_{ArH}; 2999ν_{CH}; 1599ν_{CH}; 1573$\nu_{C=C}$; 1613ν_{NO2}; 1440ν_{NO2}; LCMS-IT-TOF $[M-I]^+$ = 291 (100%), HRMS (IT TOF): m/z Calcd for $C_{18}H_{15}N_2O_2\text{-}127^+$ $[M-I]^+$: 291.1134, Found 291.1128.

2-{(*E*)-2-[4-(dimethylamino)phenyl]ethenyl}-1-methylquinolinium iodide (**3f**) 12.119 g (29.13 mmol, 83%); m.p. = 268 °C; ^1H NMR (DMSO-d_6; 400.2 MHz) δ = 3.07 (s, 6H, $2CH_3$), 4.44 (s, 3H, NCH_3), 6.81 (d, J = 8.8 Hz, 2H, aromatic), 7.54 (d, J = 15.4 Hz, 1H, vinyl), 7.84 (m, 3H, aromatic, vinyl), 8.08 (t, J = 7.5 Hz, 1H, aromatic), 8.23 (s, 1H, aromatic), 8.25 (d, J = 9.5 Hz, 1H, aromatic), 8.42 (d, J = 8.9 Hz, 1H, aromatic), 8.50 (d, J = 9.2 Hz, 1H, aromatic), 8.80 (d, J = 9.1 Hz, 1H, aromatic); $^{13}C\{^1H\}$ NMR (DMSO-d_6; 125.78 MHz) δ = 38.98, 39.68, 111.82, 118.80, 120.18, 122.38, 126.77, 127.98, 129.76, 131.96, 134.10, 139.18, 141.85, 148.89, 152.84, 156.31; lit. [24]; UV–Vis (methanol; λ [nm] (logε)): 526 (4.44), 328 (3.73), 280 (3.63), 222 (4.16), 204 (4.26); IR (KBr): 3046ν_{ArH}; 2906ν_{CH}; 1565ν_{CH}; 1529$\nu_{C=C}$; LCMS-IT-TOF $[M-I]^+$ = 289 (100%), HRMS (IT TOF): m/z Calcd for $C_{20}H_{21}N_2\text{-}127^+$ $[M-I]^+$: 289.1705, Found 289.1699.

2.4. Synthesis of vinyl N-methylated quinolinium salts. Method B

The synthesis of vinyl *N*-alkylated quinolinium salts **3g** and **3h** followed our procedure described in the literature [19–21]: **2a** (10.0 g, 35.1 mmol) was partially dissolved in Ac_2O (100 mL, 108 g, 1.06 mol), followed by the addition of appropriate benzaldehyde (50 mmol). The reaction was heated under reflux for 16 h. Then the solvent was evaporated from the resulting solution. A pyridine/H_2O system (v/v 4:1; 50 mL) was added and the reaction mixture was stirred under further reflux for 16 h. The crude product was purified by crystallization from ethanol (or methanol) and dried over P_4O_{10} to yield precipitates as follows:

2-[(*E*)-2-(2-Hydroxyphenyl)ethenyl]-1-methylquinolinium iodide (**3g**) (brick red) 1.229 g (3.16 mmol, 9%); $m.p._{dec.}$ = 228.9 °C; ^1H NMR (DMSO-*d6*; 500.18 MHz) δ = 4.53 (s, 3H, NCH_3), 6.97 (t, J = 7.5 Hz, 1H, aromatic), 7.01 (dd, J = 8.2, 0.8 Hz, 1H, aromatic), 7.36 (td, J = 8.1, 1.6 Hz, 1H, aromatic), 7.92 (dd, J = 7.9, 1.5 Hz, 1H, aromatic), 7.95 (m, 1H, aromatic), 7.97 (d, J = 16.3 Hz, 1H, vinyl), 8.18 (ddd, J = 8.8, 7.1, 1.5 Hz, 1H, aromatic), 8.24 (d, J = 16.0 Hz, 1H, vinyl), 8.37 (dd, J = 8.1, 1.3 Hz, 1H, aromatic), 8.54 (d, J = 8.9 Hz, 1H, aromatic), 8.55 (d, J = 8.8 Hz, 1H, aromatic), 9.03 (d, J = 8.9 Hz, 1H, aromatic), 10.65 (s, 1H, OH); $^{13}C\{^1H\}$ NMR (DMSO-d_6; 125.78 MHz) δ = 39.82, 116.47, 118.85, 119.25, 119.68, 121.14, 121.67, 127.69, 128.87, 129.83, 130.09, 133.02, 134.86, 139.16, 142.47, 144.10, 156.67, 157.52; UV–Vis (methanol; λ [nm] (logε)): 410 (4.09), 299 (3.78), 248 (3.74), 216 (4.20), 204 (4.17); IR (KBr): 3163ν_{ArH}; 3005ν_{CH}; 1597ν_{CH}; 1572$\nu_{C=C}$; LCMS-IT-TOF $[M-I]^+$ = 262 (100%), HRMS (IT TOF): m/z Calcd for $C_{18}H_{16}NO\text{-}127^+$ $[M-I]^+$: 262.1232, Found 262.1264.

2-[(*E*)-2-(4-Hydroxyphenyl)ethenyl]-1-methylquinolinium iodide (**3h**) (brick red) 5.598 g (14.39 mmol, 41%); $m.p._{dec.}$ = 254.4 °C; ^1H NMR (DMSO-*d6*; 400.2 MHz) δ = 4.52 (s, 3H, NCH_3), 6.92 (d, J = 8.5 Hz, 2H, aromatic), 7.71 (d, J = 15.8 Hz, 1H, vinyl), 7.90 (m, 3H, aromatic), 8.15 (t, J = 7.9 Hz, 1H, aromatic), 8.21 (d, J = 15.7 Hz, 1H, vinyl), 8.32 (d, J = 7.8 Hz, 1H, aromatic), 8.52 (d, J = 9.0 Hz, 1H, aromatic), 8.56 (d, J = 9.1 Hz, 1H, aromatic), 8.98 (d, J = 9.0 Hz, 1H, aromatic), 10.38 (s, 1H, OH); $^{13}C\{^1H\}$ NMR (DMSO-d_6; 125.78 MHz) δ = 40.18, 115.34, 116.08, 119.14, 120.69, 126.19, 127.35, 128.59, 129.92, 131.73, 134.57, 139.12, 143.26, 147.72, 156.41, 161.16; UV–Vis (methanol; λ [nm] (logε)): 424 (4.28), 398 (3.64), 260 (3.88), 217 (4.25), 203 (4.16); IR (KBr): 3421ν_{OH}; 3056ν_{ArH}; 2810ν_{CH}; 1575ν_{CH}; 1521$\nu_{C=C}$; LCMS-IT-TOF $[M-I]^+$ = 262 (100%), HRMS (IT TOF): m/z Calcd for $C_{18}H_{16}NO\text{-}127^+$ $[M-I]^+$: 262.1232, Found 262.1264.

2.5. Synthesis of (2S,R)-1-methyl-1H,1′H-2,2′-spirobi[quinoline] (**4**)

2-Aminobenzaldehyde (6.05 g, 50 mmol) was dissolved in Ac_2O (100 mL, 108 g, 1.06 mol). Subsequently, **2a** (10.0 g, 35.1 mmol) was added, and the reagents were heated under reflux for 16 h. After solvent removal by evaporating from the resulting solution, ethanol was added and the reaction mixture was stirred under reflux for 16 h, followed by filtration. To the solution H_2SO_4 (ca. 10%) was added, and the reaction mixture was stirred under reflux for 4 h. After stirring, chloroform (200 mL) was added and the resulting two-layer system was carefully brought to a neutral pH by adding aqueous KOH solution (ca. 10%). The organic layer was separated and the aqueous layer was extracted four times with chloroform. The combined organic layers were dried over $MgSO_4$. After solvent

evaporating, the crude product was purified by crystallization from the mixture of $CHCl_3$ and hexane.

2.6. Crystallography

Data for compound **2a** was collected on a KUMA KM4 diffractometer with graphite–monochromated Mo $K\alpha$ radiation using Sapphire–2 CCD detector. The apparatus was equipped with an open flow thermostat (Oxford Cryosystems) with enabled experiments at 120 K. The stream of nitrogen also prevented the specimen from contact with moisture and oxygen. The structures were solved by direct methods and refined by full–matrix least–squares on F^2 (all data) using the SHELXTL program package [25,26]. All non–hydrogen atoms were refined anisotropically. Hydrogen atoms were refined in geometrically idealised positions with isotropic temperature factors 1.2 times the equivalent isotropic temperature factor Ueq of their attached atoms (1.5 for CH_3 groups). For compounds **2b** the X-ray measurements were performed with Oxford Diffraction Gemini A Ultra diffractometer with graphite–monochromated Mo $K\alpha$ radiation ($\lambda = 0.71073$ Á). The crystal was measured at room temperature (295 K). During the data collection ω scans were performed and absorption corrections were used. The structure was solved and refined with the use of SHELX software [23]. All non–hydrogen atoms were refined with anisotropic temperature factors. All H atoms bound to C atoms were refined using a riding model with C–H distances of 0.95 Å or 0.98 Å and Uiso(H) values of 1.2Ueq(C), or 1.5 Ueq(C), respectively. H atoms, which take part in hydrogen bonds, were allowed to ride at the positions deduced from the difference maps with Uiso(H) equal to 1.2Ueq(C), 1.2Ueq(N) or 1.5Ueq(O). **2a** and **2b** crystallize in monoclinic $P2_1/n$ and $P2_1/c$ space groups. The molecular structures of the compounds are shown in Fig. 1.

The crystal data and structure refinement details are presented in Table 1. The selected distances and angles of the **2a** and **2b** compounds are collected in Table 1, and it can be seen that the values are normal.

Except the hydrogen bond linking the iodine anion and proton in position 4 in pyridine ring C(3)–H(3)···I(1) [-x ,-y, 1-z] (H···A = 2.98 Å, D···A = 3.884(3) Å and D–H···A angle 165.0°) in the crystal structures, **2a** and **2b** form the π-stacking interactions as one can see in Fig. 2.

There are interactions between the phenyl C(4)–C(9) and pyridine N(1)–C(1)–C(9) rings in the molecules, which are generated by 1–x, -y, 1-z and -x; -y; 1-z symmetry operations in **2a** and –x, 1-y,1-z and 1-x,1-y,1-z in **2b**. The centroid–centroid distances vary from 3.80 Å and 3.94 Å (phenyl rings) to 3.50 Å and 3.54 Å (pyridine rings) and the shift distances are in the range 1.98, 1.42 Å to 1.00, 0.94 Å in **2a** and **2b**, respectively. Our observations are consistent with A. N. Swinburne et al. work [5].

2.7. Instrumentation

NMR spectra were obtained with Bruker Avance 400 operating at 400.13 MHz (^{1}H) and 100.4 MHz (^{13}C) at 30 °C; chemical shifts referenced to ext. TMS (^{1}H, ^{13}C); positive signs of chemical shifts denote shifts to lower frequencies, coupling constants are given as absolute values. Melting points are uncorrected.

3. Results and discussion

The synthesis of *N*-alkylated quinolinium salts (**2**) based on the reaction of **1a** and **1b** with appropriate RI (R = CH_3, Et, CH_2CHCH_2, Bu^i) were carried out under reflux with a set of identical reaction conditions (Scheme 1) according to already published methodology [16,17,22,23]. Reactions were successful even in multigram scale with isolated yields up to 78%, except **2d** (5%). The pattern of the yield distribution depends on the substituent location on the pyridinium ring through steric and/or electronic effect. The reaction presented on Scheme 1 showed that the impact on the nitrogen atom reactivity is not only from methyl group on C2, but also from methoxy group on peri position (C8) for **2d**.

The synthesis of **3** was based on the reactions of **2a** with appropriate benzaldehyde, which were carried out under reflux with a set of identical reaction conditions (Scheme 2). The pattern of the yield distribution depends on isolation procedure. Compounds with low solubility were easily precipitated giving higher isolation yield up to 83% for **3f**. Two protocols for the synthesis of **3** were elaborated. Firstly method A was designed for compounds possessing non-nucleophilic substituents, such as halogens or nitro. Secondly, method B was dedicated for molecules with nucleophilic substituents such as hydroxyl or amino functional groups based on already published methodology [19–21].

From the theoretical point of view, positive charges for both carbons atoms C2 and C4 (ortho and para positions) should be expected, which is correct for **2b** (0.664 and 0.199, respectively). However, for **2a** only C2 has positive charge (0.371), C4 has negative charge, close to zero (–0.093) (Fig. 3). The atomic charge calculations for **2a** and **2b** showed that methylated nitrogen atom had

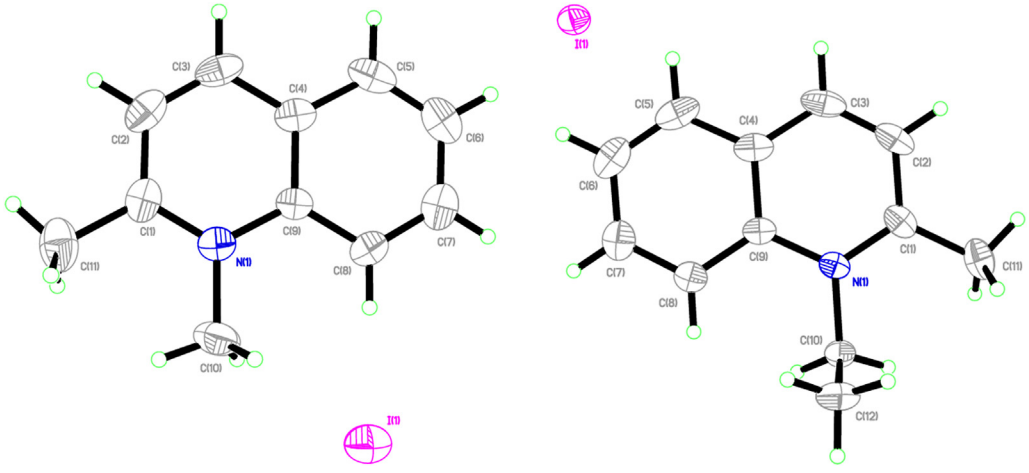

Fig. 1. ORTEP drawing of **2a** (right) and **2b** (left) with 30% probability displacement ellipsoids.

Table 1
Crystal data and structure refinement details of **2a** and **2b** compounds.

	2a	**2b**
Empirical formula	$C_{11}H_{12}N$, I	$C_{12}H_{14}N$, I
Formula weight	285.12	299.14
Temperature [K]	120(2)	295(2)
Crystal system	Monoclinic	Monoclinic
Space group	$P2_1/n$	$P2_1/c$
Unit cell dimensions		
a [Å]	6.8937(3)	7.1855(3)
b [Å]	10.1321(4)	15.9261(5)
c [Å]	15.9019(6)	10.3344(4)
β	96.871(4)	94.722(3)
V [Å^3]	1102.74(8)	1178.62(7)
Z	4	4
Calculated density [Mg/m^3]	1.717	1.686
Mo–K$_\alpha$ λ [Å]	0.71073	0.71073
Absorption coefficient [mm^{-1}]	2.860	2.680
F(000)	552	584
Crystal dimensions [mm]	0.12 × 0.09 × 0.05	0.19 × 0.10 × 0.08
θ range for data collection [°]	3.38 to 25.05	3.57 to 25.05
Index ranges	$-8 \le h \le 8$ $-12 \le k \le 12$ $-18 \le l \le 18$	$-8 \le h \le 8$ $-18 \le k \le 18$ $-12 \le l \le 12$
Reflections collected	19,810	6826
Independent reflections	1952 [$R_{(int)} = 0.0288$]	2086 [$R_{(int)} = 0.0264$]
Data/restraints/parameters	1952/0/120	2086/0/129
Goodness-of-fit on F^2	1.073	1.049
Final R indices [I > 2σ(I)]	$R_1 = 0.0207$ w$R_2 = 0.0539$	$R_1 = 0.0234$ w$R_2 = 0.0491$
R indices (all data)	$R_1 = 0.0252$ w$R_2 = 0.0546$	$R_1 = 0.0319$ w$R_2 = 0.0518$
Largest diff. Peak and hole [e Å^{-3}]	0.313 and −0.561	0.345 and −0.532
CCDC number	795822	873830

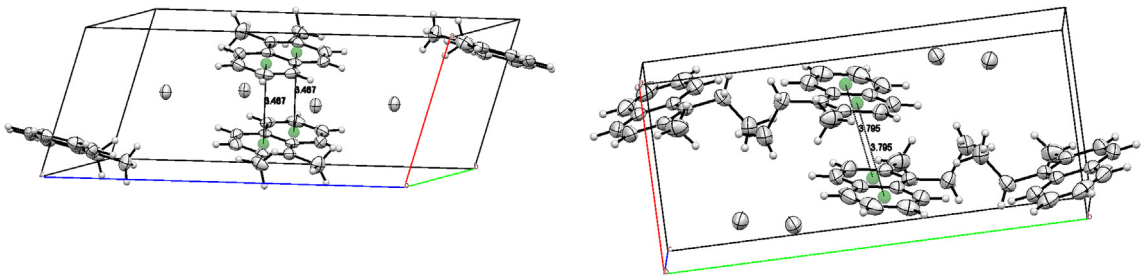

Fig. 2. The π-stacking interactions in the structures of **2a** (right) and **2b** (left).

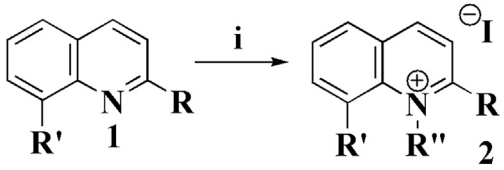

Compound	R	R'	R''	Yield (%)
2a	Me	-	Me	75
2b	Me	-	Et	71
2c	Me	-	Bu^i	14
2d	-	OMe	Me	5
2e	Me	-	CH_2CHCH_2	78

Scheme 1. Synthesis of **2**. Reagents and conditions: (i); R″I, reflux, 16 h.

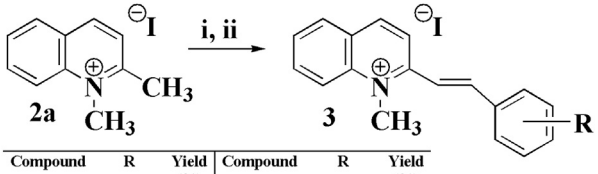

Compound	R	Yield (%)	Compound	R	Yield (%)
3a	C2-Cl	13	**3e**	C4-NO_2	78
3b	C4-Cl	13	**3f**	C4-NMe_2	83
3c	C4-Br	56	**3g**	C2-OH	9
3d	C4-OMe	31	**3h**	C4-OH	41

Scheme 2. Synthesis of **3**. Reagents and conditions: (i); Ac_2O, appropriate benzaldehyde, reflux (ii); PY, H_2O, reflux.

positive charge (0.199) for **2b**, and has negative charge (−0.472) for **2a**.

The presence of positively charged carbon atom C2, which is close to positive charged methylated nitrogen atom, could have an impact on their chemical reactivity. The deprotonation of hydroxyl or amino group located on ortho position on the phenyl ring of vinyl *N*-methylated quinolinium salts **3g** and **3h** analogues could introduce intramolecular cyclization led to spiro type compounds **4**, which was postulated by Zakhs et al. (Scheme 3) [30,31]. For hydroxyl or amino group located on para or meta position on phenyl ring **3**, a condensation reaction should lead to polymeric material.

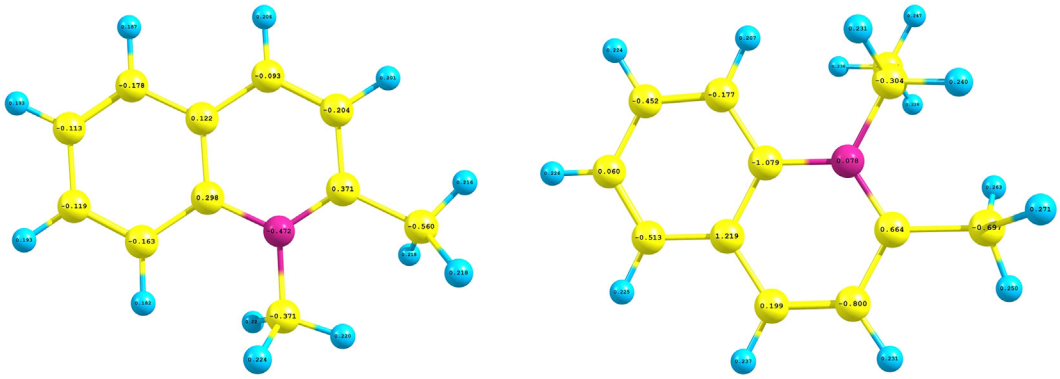

Fig. 3. Natural atomic charges of **2a** (left) and **2b** (right).

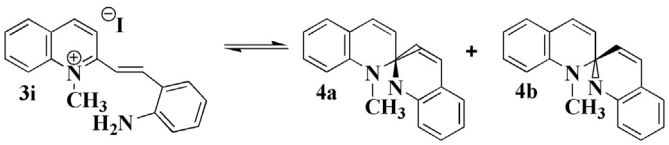

Scheme 3. Synthesis of (2*S*,*R*)-1-methyl-1*H*,1′*H*-2,2′-spirobi[quinoline] (**4**). Both **4a** an **4b** showed helical chirality.

The presence of racemic **4a** and **4b** were proved by NMR techniques (see below).

3.1. NMR

The ^{1}H NMR and ^{13}C NMR solution spectra of **2** and **3** showed distinctive H-1 and C-13 signals from C2–CH_3 and *N*-CH_3 functional groups (Table S1, Supplementary data). The experimental ^{1}H and ^{13}C chemical shifts of aromatic carbons and protons of **2** in DMSO-*d6* possess almost the same values. The analysis of the trends in ^{1}H chemical shifts of vinyl functional group in **3** revealed that the electron donating substituents such as methoxy (**3d**), dimethylamino (**3f**) or hydroxyl (**3g**, **3h**) on phenyl group in the constitution of **3** significantly increased the shielding effect (upfield effect, smaller δ), resulting in the decreased chemical shifts of selected H-1 signals in comparison with nitro group (**3e**). The analysis of the value of coupling constants (ca. 16 Hz) for vinyl protons confirmed the sole presence of *E* conformer (Table S2, Supplementary data). For signal assignments, heteronuclear 2D ^{1}H–^{13}C spectra heteronuclear multiple quantum correlation (HMQC) and heteronuclear single quantum correlation (HSQC) were used. The analysis of the ^{1}H NMR and ^{13}C NMR spectra in basic solvents such as KOD/D_2O/DMSO-*d6* by comparing with neutral DMSO-*d6* revealed that the hydroxyl derivatives and their amino analogues of vinyl *N*-methylated quinolinium salts **3g** and **3h** could form spiro type structure through intramolecular and intermolecular condensation reaction (Scheme 3). The coupling constants (ca. 3 Hz only from crude reaction mixture) of vinyl protons indicated presence of *Z* conformer, the spiro type compounds **4**. For signal assignments, heteronuclear 2D ^{1}H–^{13}C spectra heteronuclear multiple quantum correlation (HMQC) and heteronuclear single quantum correlation (HSQC) were used (Fig. 4).

3.2. IR

The IR spectra of the compounds are similar, and Fig. 5 presents the spectrum of **2a** as example. The characteristically sharp and strong bands with maxima close to 1600 cm^{-1} and in the range 1521 cm^{-1} to 1598 cm^{-1}are assigned to the stretches of C=N and C=C in quinoline ring (Table 3). In the case of **3d**, the stretching vibration of the C=C double bond on vinyl moiety gives band at 1745 cm^{-1}, and the shift is connected with methoxy group in para position in the phenyl ring.

3.3. DFT calculations and electronic spectra

The calculations were carried out by using Gaussian 09 [27] program. The DFT/B3LYP [28] method was used for the geometry optimization and electronic structure determination. The geometry optimization was made for gas phase molecule in both cationic and neutral forms. For each form a frequency calculation was carried out, verifying that the optimized molecular structure obtained corresponds to energy minimum, thus only positive frequencies were expected. The calculations were performed using the polarization functions for all atoms: 6-31G** – carbon, nitrogen, hydrogen and Lanl2dz ECP [29] for iodine.

The geometry of **2a** and **2b** were optimized in singlet states using the DFT method with the B3LYP functional. Some optimized geometric parameters of the compounds are listed in Table 1. Comparing the theoretical data with the experimental values indicates that optimized bond lengths and angle values are slightly different with the experimental results. It should be noted that the geometry of the solid state structure is subject to intra and intermolecular interactions, such as hydrogen bonding and van der Waals interactions. As seen in Table 2, the largest discrepancies between the calculated and experimental geometrical parameters are observed in N(1)–C(1) and C(1)–C(11) bonds. The largest difference between experimental and calculated DFT bond length is 0.03 Å which suggest that the calculation precision is satisfactory. Similar situation is also observed for calculated bond angles with DFT method. The good agreement between experimental IR spectrum and the calculated IR frequencies, as one can see on the Fig. 5, also confirms the optimized geometry of the compound. Both electronic structures of the compound were calculated for cationic and neutral forms. Since the frontier HOMOs in the neutral forms of the compounds are located on the *p* orbital of iodine anion (see Fig. 6), the HOMO→LUMO transitions have charge transfer characteristics.

The first, lowest energy, bands on the UV–Vis spectra of **2a**, **2b** and **2c** are in the UV region (320 nm); in the case of the vinyl compounds the maxima are shifted to lower energy due to the extended conjugated double bonds system. Moreover the UV–Vis spectra of the **3d**, **3g**, **3h** as well as **2d** compounds present maxima on the visible region (above 400 nm) what is associated with the presence of electron donating substituents, as methoxy or hydroxyl groups, in the molecules of these compounds. The comparison

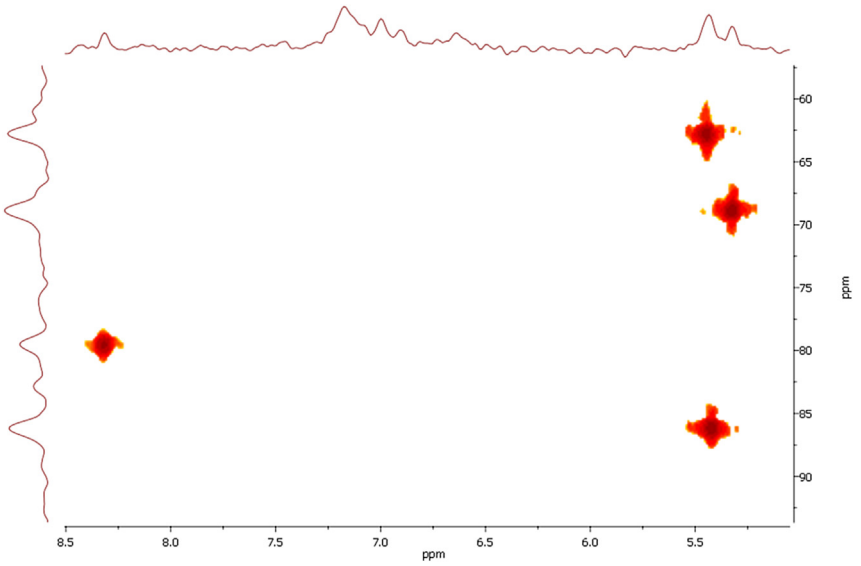

Fig. 4. HMQC spectrum of **4**, vinyl region.

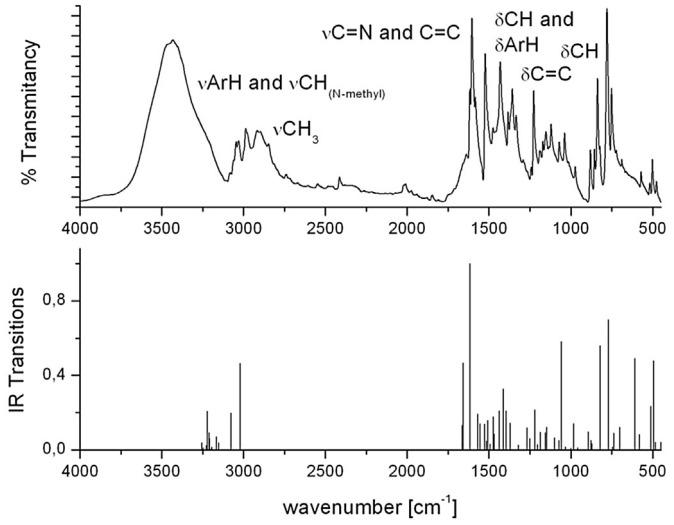

Fig. 5. The experimental and calculated IR spectra of **2a**.

between the spectra of **3a** and **3b** as well as **3g** and **3h** compounds shows the difference between substituents located on ortho and para position in benzene ring. The substituents in para-position exert higher impact on electronic structure than one in 2 positions in the ring. The chloride in position 4 exerts more donating impact than ortho substituent. The replacement of chloride for **3b** into bromide for **3c** does not change the maximum of the lowest energy band whereas increases the intensity of the band. The energies of HOMOs, LUMOs and electronic gaps for cationic quinolone moieties present Fig. 7.

4. Conclusion

In the present studies, we reported the synthesis and spectroscopic characterization of selected crystalline π-conjugated vinyl *N*-alkylated quinolinium salts (**2**) and their precursor's *N*-alkylated quinolinium salts (**3**) using IR, UV–Vis and multinuclear NMR spectroscopic techniques. Both of **2a** and **2b** have been characterized by single crystal X-ray diffraction method. X-ray crystal structure analysis of **2a** and **2b** showed the presence of the π-stacking interactions. The ^{1}H and ^{13}C NMR spectra of presented

Table 2
Selected bond lengths and angles for **2a** and **2b** (Å and °).

	2a		**2b**	
	exp	calc	exp	calc
Bond lengths [Å]				
N(1)—C(1)	1.335(3)	1.361	1.341(3)	1.355
N(1)—C(9)	1.394(3)	1.402	1.396(3)	1.400
N(1)—C(10)	1.475(3)	1.469	1.494(3)	1.496
C(1)–C(2)	1.402(4)	1.424	1.398(4)	1.408
C(1)–C(11)	1.484(4)	1.509	1.486(4)	1.505
C(4)—C(9)	1.405(4)	1.422	1.414(4)	1.429
C(4)—C(3)	1.406(4)	1.424	1.399(4)	1.412
C(4)—C(5)	1.417(4)	1.412	1.417(4)	1.420
C(6)—C(7)	1.387(4)	1.404	1.400(5)	1.413
C(8)—C(9)	1.396(4)	1.409	1.402(4)	1.414
C(10)—C(12)			1.516(4)	1.530
Bond angles [°]				
C(1)—N(1)—C(9)	122.0(2)	121.4	121.9(2)	121.8
C(1)—N(1)—C(10)	120.5(2)	119.5	119.9(2)	119.5
C(9)—N(1)—C(10)	117.6(2)	117.9	118.2(2)	118.7
N(1)—C(1)—C(11)	121.1(3)	120.3	121.0(3)	120.8
N(1)—C(10)—C(12)			110.7(2)	112.7

Table 3
Selected vibrational frequencies of studied **2** and **3**.

	ν_{OH}	ν_{ArH}	ν_{CH}	$\nu_{C=C}$; $\nu_{C=N}$	ν_{O-CH3}	ν_{NO2}
2a		3045	2986; 2916	1604; 1582		
2b		3059	2924	1602; 1579		
2c		3097	2957	1618; 1598		
2d		3097	2955, 2853	1598; 1536	1049	
2e		3035	2925	1603; 1525		
3a		3063	2960	1608; 1585		
3b		3060	3012	1603; 1571		
3c		3050	3023	1607; 1574		
3d		3068	2955; 2832	1745; 1588	1173	
3e		3065	2999	1599; 1573		1613; 1440
3f		3046	2906	1565; 1529		
3g		3163	3005	1597; 1572		
3h	3421	3056	2810	1575; 1521		

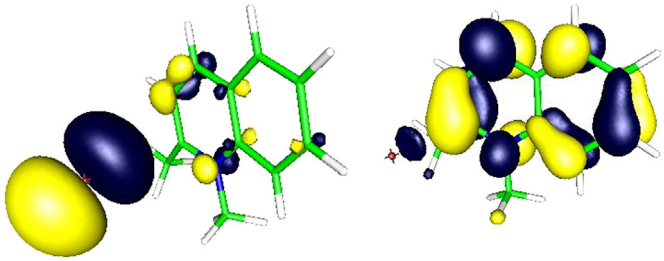

Fig. 6. Contours of HOMO (left) and LUMO (right) orbitals of **2a**.

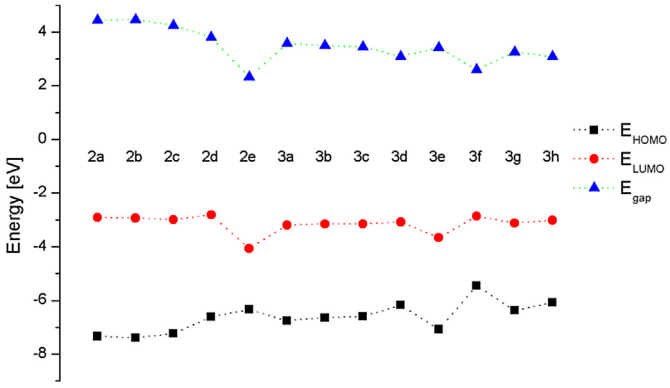

Fig. 7. Calculated energies of HOMOs, LUMOs and the gap in the cationic forms of the compounds.

compounds displayed distinctively diagnostic signals from C2–CH_3 and *N*-Alkyl functional groups. The analysis of the value of coupling constants for vinyl protons confirmed the sole presence of *E* conformer for **3** and *Z* for spiro type compounds **4**. This unprecedented reaction leading to spiro type compounds **4** is likely a forerunner of a series interesting substrates, not only to their analogy to spiroindolones, also a new and potent chemotype for the treatment of malaria. Further structural and biological studies are in progress.

Acknowledgments

The GAUSSIAN09 calculations were carried out in the Wrocław Centre for Networking and Supercomputing, WCSS, Wrocław, Poland (http://www.wcss.wroc.pl grant number 18).

Appendix A. Supplementary data

Supplementary data related to this article can be found at http://dx.doi.org/10.1016/j.molstruc.2015.11.011.

References

[1] A. Schmidt, Adv. Heterocycl. Chem. 85 (2003) 67–171.
[2] J.W. Lee, M. Jung, G.R. Rosania, Young-Tae Chang, Chem. Commun. (2003) 1852–1853.
[3] S. Jayaraman, A.S. Verkman, Biophys. Chem. 85 (2000) 49–57.
[4] J. Najbar, R.C. Dorfman, M.D. Fayer, J. Chem. Phys. 94 (1991) 1081–1092.
[5] A.N. Swinburne, M.J. Paterson, A. Beeby, J.W. Steed, Org. Biomol. Chem. 8 (2010) 1010–1016.
[6] A. Schmidt, T. Mordhorst, M. Nieger, Org. Biomol. Chem. 3 (2005) 3788–3793.
[7] A. Busetti, D.E. Crawford, M.J. Earle, M.A. Gilea, B.F. Gilmore, S.P. Gorman, G. Laverty, A.F. Lowry, M. McLaughlin, K.R. Seddon, Green Chem. 12 (2010) 420–425.
[8] M. McLaughlin, M.J. Earle, M.A. Gîlea, B.F. Gilmore, S.P. Gorman, K.R. Seddon, Green Chem. 13 (2011) 2794–2800.
[9] J. Zou, P.S. Mariano, Photochem. Photobiol. Sci. 7 (2008) 393–404.
[10] M. Hanaoka, C. Mukai, K. Nagami, K. Okajima, S. Yasuda, Chem. Pharm. Bull. 32 (1984) 2230–2240.
[11] J.-L. Vasse, V. Levacher, J. Bourguignon, G. Dupas, Chem. Commun. (2002) 2256–2257.
[12] N.S. Scrutton, A.R.C. Raine, Biochem. J. 319 (1996) 1–8.
[13] N. Zacharias, D.A. Dougherty, Trends Pharmacol. Sci. 23 (2002) 281–287.
[14] J.P. Gallivan, D.A. Dougherty, Proc. Natl. Acad. Sci. U. S. A. 96 (1999) 9459–9464.
[15] S. Yamada, Org. Biomol. Chem. 5 (2007) 2903–2912.
[16] B.K. Sarangi, R.K. Behera, J. Indian Chem. Soc. 62 (1985) 759–762.
[17] H. Russ, W. Engel, E. Schömig, J. Med. Chem. 36 (1993) 4208–4213.
[18] G. Malecki, J.E. Nycz, E. Ryrych, L. Ponikiewski, M. Nowak, J. Kusz, J. Pikies, J. Mol. Struct. 969 (2010) 130–138.
[19] L. Ponikiewski, J.E. Nycz, Acta Cryst. E E65 (2009) o515–o530.
[20] W. Cieslik, R. Musiol, J.E. Nycz, J. Jampilek, M. Vejsova, M. Wolff, B. Machura, J. Polanski, Bioorg. Med. Chem. 20 (2012) 6960–6968.
[21] R. Musiol, J. Jampilek, J.E. Nycz, M. Pesko, J. Carroll, K. Kralova, M. Vejsova, J. O'Mahony, A. Coffey, A. Mrozek, J. Polanski, Molecules 15 (2010) 288–304.
[22] J. Jaroszewska, I. Wawer, J. Oszczapowicz, Org. Magn. Reson. 22 (1984) 323–327.
[23] L. Tan, W. Lin, S. Zhu, L. Yuan, K. Zheng, Org. Biomol. Chem. 12 (2014) 4637–4643.
[24] L.L. Seiad, D. Villemin, N. Bar, N. Hachemi, Synth. Commun. 42 (2012) 650–657.
[25] G.M. Sheldrick, SHELXTL-97, University of Göttingen, 1997.
[26] G.M. Sheldrick, Acta Cryst. A64 (2008) 112–122.
[27] M.J. Frisch, G.W. Trucks, H.B. Schlegel, G.E. Scuseria, M.A. Robb, J.R. Cheeseman, G. Scalmani, V. Barone, B. Mennucci, G.A. Petersson, H. Nakatsuji, M. Caricato, X. Li, H.P. Hratchian, A.F. Izmaylov, J. Bloino, G. Zheng, J.L. Sonnenberg, M. Hada, M. Ehara, K. Toyota, R. Fukuda, J. Hasegawa, M. Ishida, T. Nakajima, Y. Honda, O. Kitao, H. Nakai, T. Vreven, J.A. Montgomery Jr., J.E. Peralta, F. Ogliaro, M. Bearpark, J.J. Heyd, E. Brothers, K.N. Kudin, V.N. Staroverov, R. Kobayashi, J. Normand, K. Raghavachari, A. Rendell, J.C. Burant, S.S. Iyengar, J. Tomasi, M. Cossi, N. Rega, J.M. Millam, M. Klene, J.E. Knox, J.B. Cross, V. Bakken, C. Adamo, J. Jaramillo, R. Gomperts, R.E. Stratmann, O. Yazyev, A.J. Austin, R. Cammi, C. Pomelli, J.W. Ochterski, R.L. Martin, K. Morokuma, V.G. Zakrzewski, G.A. Voth, P. Salvador, J.J. Dannenberg, S. Dapprich, A.D. Daniels, O. Farkas, J.B. Foresman, J.V. Ortiz, J. Cioslowski, D.J. Fox, Gaussian 09, Revision A.1, Gaussian, Inc., Wallingford CT, 2009.
[28] A.D. Becke, J. Chem. Phys. 98 (1993) 5648–5752.
[29] C.E. Check, T.O. Faust, J.M. Bailey, B.J. Wright, T.M. Gilbert, L.S. Sunderlin, J. Phys. Chem. A 105 (2001) 8111–8116.
[30] V.P. Martynova, N.E. Shelepin, N.S. Loseva, É.R. Zakhs, L.E. Nivorozhkin, V.I. Minkin, L.S. Éfros, Khim. Geterotsikl. (1970) 152–154.
[31] E.V. Bashutskaya, É.R. Zakhs, L.S. Éfros, Khim. Geterotsikl. (1975) 969–975.